A Tunable Dispersion Compensating MEMS All-Pass Filter

C. K. Madsen, *Senior Member, IEEE*, J. A. Walker, J. E. Ford, K. W. Goossen, *Member, IEEE*, T. N. Nielsen, and G. Lenz

***Abstract*—A tunable dispersion compensating filter based on a multistage optical all-pass filter with a microelectromechanical (MEM) actuated variable reflector and a thermally tuned cavity is described. A two-stage device was demonstrated with a tuning range of ±100 ps/nm, 50-GHz passband and a group delay ripple less than ±3 ps. The device has negligible polarization dependence and is suitable for single or multiple channel compensation. An off-axis, two-fiber package with an excess loss <2 dB/stage avoids the need for a circulator. By cascading four stages, a passband to channel spacing ratio of 0.8 is obtained that allows both 40 Gb/s nonreturn-to-zero (NRZ) and return-to-zero (RZ) signals to be compensated.**

I. Introduction

TUNABLE chromatic dispersion compensation is critical for high bitrate lightwave systems. Reconfigurable optical networks introduce a need for tunable dispersion compensation since different routes may have different cumulative dispersions. Nonlinear systems have an optimal dispersion that depends on the channel power [1], which may vary over time. Previous all-pass filter work used a Gires–Tournois Interferometer (GTI) to compensate a fixed dispersion [2] over a small passband width (5 GHz). The GTI is essentially a single-stage all-pass filter consisting of a Fabry–Perot cavity with one mirror having ∼100% reflectivity. In this letter, we describe a completely tunable all-pass filter based on a microelectromechanically actuated partial reflector, and we demonstrate multistage filter designs, which are required to increase the filter passband width and dispersion [3], [4].

II. Device Design and Operation

The tunable all-pass filter is based on the mechanical antireflection switch (MARS) device [5], [6], which is a variable-thickness Fabry–Perot cavity consisting of a silicon substrate, an air gap, and a quarter-wave thick dielectric membrane. A silicon nitride layer is used for the membrane, and the gap is nominally $3\lambda_0/4$. The cavity formed by the membrane and top surface of the substrate yields a reflection of about 70%. The gap is varied from $3\lambda_0/4$ to $\lambda_0/2$ by applying a voltage to electrodes on top of the membrane as shown in Fig. 1. The voltage creates an electrostatic force that pulls the membrane closer to the substrate surface, while the membrane tension provides a linear restoring force. At a gap of $\lambda_0/2$, the reflection is reduced to ∼0% since the silicon nitride acts as an antireflection coating for the silicon substrate. To make an all-pass filter, we use the Fabry–Perot cavity as a tunable, partial reflector and add a high reflectance coating to the back side of the substrate. A reflectivity >97% is obtained using a multi-layer stack. The substrate thickness L determines the free spectral range FSR $= c/2n_gL$, where n_g is the group index. For a 100-GHz FSR, the silicon thickness is 411 μm. To minimize diffraction losses, a large expanded beam (∼300 μm waist) and drum size (1.25 mm diameter) were used. Note that the peak membrane deflection, 0.35 μm, is quite small compared to the drum diameter.

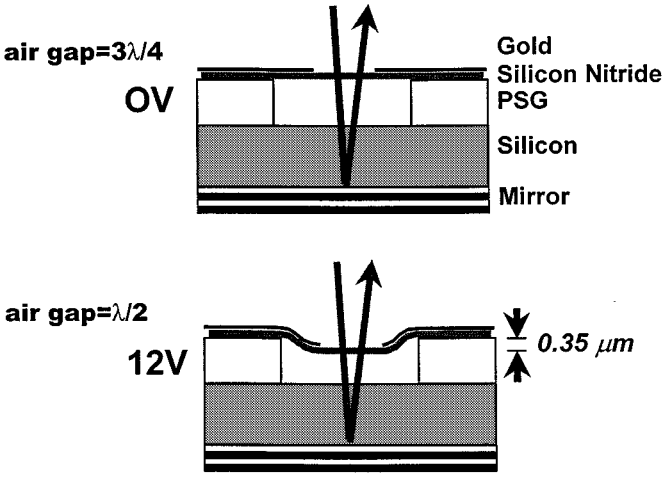

Fig. 1. MEMS all-pass filter schematic showing the change in air gap with applied voltage.

The device package for a single-stage filter consists of two fibers, a lens and the all-pass filter. The input and output fibers are offset from the lens axis so that the reflected light from the device couples into the output fiber. A small incidence angle (∼0.6°) was chosen to minimize the walkoff between multiple reflections and the polarization dependent loss. An on-axis package with a single fiber attachment was also demonstrated using a circulator to separate the input and output light.

The group delay for an N-stage, lossless all-pass filter is $\tau(\omega) = T\sum_{n=1}^{N}(1-\rho_n^2)/(1+\rho_n^2-2\rho_n\cos(\omega T-\phi_n))$ where ρ_n and $\phi_n = (2\pi/\lambda)\Delta_n$ are the partial amplitude reflectance and phase of the nth stage, respectively. The optical path length deviation from the nominal value is $\Delta_n = 2(n_nL_n - nL)$, and $T = 1/\mathrm{FSR}$ is the unit delay. The all-pass filter provides a frequency-dependent group delay that is periodic. By choosing the filter period to equal the channel spacing in a WDM system, multiple channels can be compensated. The filter dispersion is $D = d\tau/d\lambda$ (ps/nm). For a completely tunable all-pass filter,

Manuscript received January 6, 2000; revised February 16, 2000.

The authors are with Bell Labs, Lucent Technologies, Murray Hill, NJ 07974 USA (e-mail: cmadsen@lucent.com).

Publisher Item Identifier S 1041-1135(00)04628-0.

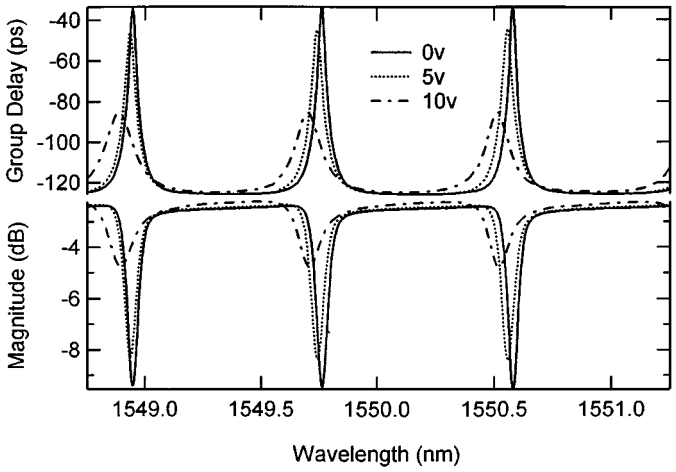

Fig. 2. Single-stage group delay and magnitude response for three applied voltages.

both the partial reflector and the cavity optical length must be tunable. By varying the applied voltage, the partial reflectance of the front mirror is changed. To tune ϕ_n, the substrate is mounted on a thermo-electric cooler, and the cavity optical thickness is tuned via the thermo-optic effect. Tuning of the cavity length can also be used to compensate for variations in the fabricated cavity length from the design nominal.

III. Experimental Results

The group delay was measured using the phase shift technique and stepping a tunable laser in 0.01 nm increments. The group delay characteristics for several voltage settings of a single-stage device are shown in Fig. 2 over three periods of the response. At 0 V, the large partial reflectance yields a narrow peak in the group delay response with a large delay at resonance, while lower partial reflectance values have a broader response with a smaller peak delay. For dispersion compensation, lower partial reflectivities are desirable as discussed below. In a lossless filter, the magnitude response is a constant. Because of the finite loss per round-trip in the cavity, the device has a wavelength dependent loss that varies with applied voltage as shown in Fig. 2. By fitting the partial reflectivity and round-trip cavity loss to the group delay and magnitude spectra of a single stage, the cavity round-trip loss is estimated to be 0.6 dB. (The same cavity loss was obtained for the single fiber package with a circulator, indicating that off-axis illumination is not the major loss source.) The excess package loss for several devices was between 1.3 and 2 dB and the polarization dependent loss was negligible ($<$0.1 dB). The filter parameters change very little over a broad wavelength range since the cavity dispersion is small and the partial reflector has only a small wavelength dependence. For example, an optical low coherence measurement at 7.5 V gave $\rho = 0.53 \pm 0.02$ over a 32-nm range. The partial reflectivity reaches a minimum around 12 V, where the delay and loss spectra are essentially constant.

For compensating the dispersion of optical fibers, a linear group delay response is needed across the channel passband. The group delay ripple is defined as the difference in the desired linear group delay and the filter's delay. A single-stage filter has a limited bandwidth (or portion of the FSR) over which a linear response can be approximated. The bandwidth decreases as the dispersion increases, and vice versa. By using two stages, the dispersion for the same bandwidth and ripple is doubled. Each stage has a different partial reflector, and a particular relative phase between the two cavities is required. The design parameters for a two-stage filter with a 50 GHz passband width over which the group delay error is equiripple are shown in Table I. A 100 GHz FSR was assumed. The peak dispersion, group delay ripple, and average filter delay are indicated. Note that the peak power reflectivities ρ^2 are less than 33%.

TABLE I
Design Parameters for a Two-Stage All-Pass Filter with a 100 GHz FSR, 50 GHz Passband Width, and Equiripple Group Delay Error

D (ps/nm)	Ripple (ps peak)	τ_{avg} (ps)	ρ_1	ρ_2	ϕ_1 (radians)	ϕ_2 (radians)
-50.0	0.43	22.5	0.388	0.229	-1.545	-3.048
-75.0	1.12	24.5	0.491	0.328	-1.652	-2.960
-100.0	2.32	26.3	0.570	0.419	-1.710	-2.891

The measured group delay response for a two-stage filter at several different parameters settings is shown in Fig. 3. First, the partial reflectance as a function of voltage and the resonant wavelength versus temperature were determined for each stage. Then, the voltage and temperature for each stage were set to obtain the design values for ρ_n and ϕ_n, and the overall response of the two-stage filter was measured. In Fig. 3(a), the parameters from the $D = -100$ ps/nm design in Table I were used. The delay spectra for each stage, the overall filter delay, the linear fit across a 50-GHz passband, and the group delay ripple are shown. The dispersion and ripple are in close agreement with the design values in Table I. Note the six extrema in the ripple behavior, which is in agreement with the $2N + 2$ extrema required in theory where N is the number of stages. The round-trip cavity loss introduces a loss variation of 3.1 dB across the passband. By reducing the round-trip cavity loss, the loss variation will also be reduced. By changing the relative phases of the two stages (substituting $-\phi_n$ in Table I), an equivalent positive dispersion can be obtained with the same bandwidth and ripple [see Fig. 3(b)]. By simultaneously varying the phases and applied voltages, the dispersion can be tuned between positive and negative values over a total range of 200 ps/nm. A larger dispersion can be achieved by reducing the passband width over which low group delay ripple is required. A design for a 30-GHz passband with 200 ps/nm dispersion was implemented as shown in Fig. 3(c).

The dispersion tuning range required to optimally compensate a nonlinear system whose launch powers vary in time is small [7]. As reported by Nielsen *et al.*, a 60-ps/nm variation was sufficient to cover an 8-dB range of launch powers for a 40-Gb/s nonreturn-to-zero (NRZ) signal and improve the receiver sensitivity by several dB over a fixed compensator. The dispersion tuning ranges demonstrated experimentally are more than adequate for such an application, but we must increase the passband width by either decreasing the dispersion tuning range or increasing the number of stages. As an example, a four-stage

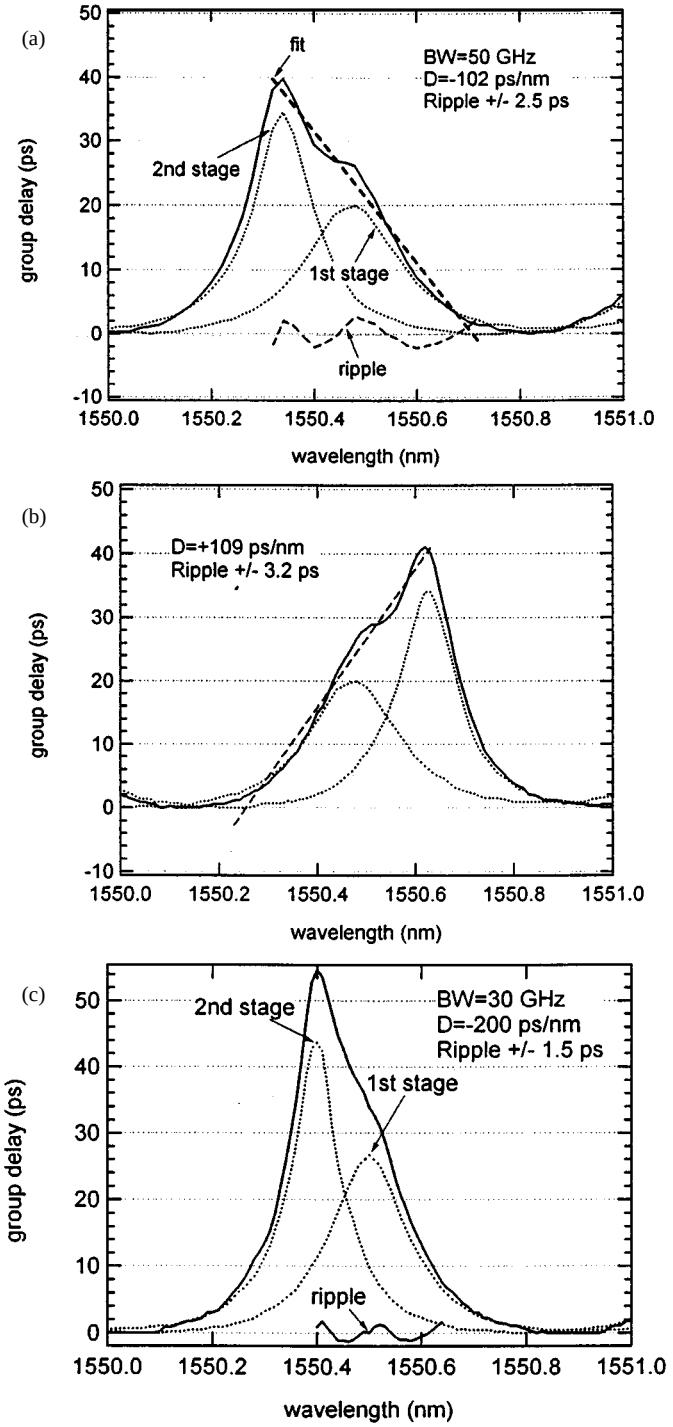

Fig. 3. Group delay and group delay ripple for a two-stage device with a dispersion of (a) −102 ps/nm, (b) +109 ps/nm, and (c) −200 ps/nm.

filter with a 100-GHz FSR and 80-GHz passband was designed. For a peak dispersion of 100 ps/nm, the group delay ripple was ±4 ps. Linear system simulations for 40-Gb/s NRZ and return-to-zero (RZ) were performed using the filter to compensate for 100 ps/nm of fiber dispersion. The receiver sensitivity relative to the back-to-back performance was calculated as a function of the channel center wavelength. A cavity loss of 0.5 dB was assumed for the filter. Tolerance windows of 0.2 and 0.3 nm were obtained for the RZ and NRZ signals, respectively, with less than 1 dB penalty.

IV. Conclusion

We fabricated a fully tunable, all-pass filter with a 100 GHz FSR and negligible polarization dependence. Using a two-stage device, a tuning range of ±100 ps/nm, a passband width of 50 GHz, and a group delay ripple of <3-ps peak were demonstrated. The measured and theoretical group delay response agree to within the measurement uncertainty, showing that higher order filters are practical. The MEM's all-pass filter is easily scaled to other FSR's by changing the substrate thickness; whereas, planar waveguide ring resonator implementations [4] require about a factor of two increase in the core-to-cladding refractive index difference to limit bend loss for a factor of two increase in the FSR. Unlike the MEM's devices discussed here, planar ring resonators are easily cascaded but currently suffer from waveguide birefringence, which introduces polarization mode dispersion.

References

[1] B. Eggleton, J. Rogers, P. Westbrook, T. Strasser, T. Nielsen, P. Hansen, and K. Dreyer, "Electrically tunable power efficient dispersion compensating fiber Bragg gratings for dynamic operation in nonlinear lightwave systems," in *Proc. Optic. Fiber Commun. Conf. Int. Conf. Integr. Opt. Optic. Fiber Commun.*, San Diego, CA, Feb. 23–26, 1999, Postdeadline PD27.

[2] A. Gnauck, L. Cimini, J. Stone, and L. Stulz, "Optical equalization of fiber chromatic dispersion in a 5-Gb/s transmission system," *IEEE Photon. Technol. Lett.*, vol. 2, pp. 585–587, Aug. 1990.

[3] C. Madsen and G. Lenz, "Optical allpass filters for phase response design with applications for dispersion compensation," *IEEE Photon. Technol. Lett.*, vol. 10, pp. 994–996, July 1998.

[4] C. K. Madsen, G. Lenz, A. J. Bruce, M. A. Cappuzzo, L. T. Gomez, and R. E. Scotti, "Integrated all-pass filters for tunable dispersion and dispersion slope compensation," *IEEE Photon. Technol. Lett.*, vol. 11, pp. 1623–1625, Dec. 1999.

[5] K. Goossen, J. Walker, and S. Arney, "Silicon modulator based on mechanically-active antireflection layer with 1 Mbit/sec capability for fiber-in-the-loop applications," *IEEE Photon. Technol. Lett.*, vol. 6, pp. 1119–1121, Sept. 1994.

[6] J. Ford and J. Walker, "Dynamic spectral power equalization using micro-opto-mechanics," *IEEE Photon. Technol. Lett.*, vol. 10, pp. 1440–1442, Oct. 1998.

[7] T. Nielsen, B. Eggleton, J. Rogers, P. Westbrook, P. Hansen, and T. Strasser, "Fiber bragg grating tunable dispersion compensator for dynamic post dispersion optimization at 40 Gbit/s," in *Proc. Eur. Conf. Optic. Commun.*, Nice, France, 1999, p. I-34.